Supplementary information

Photodynamic treatment of multidrug-resistant bacterial infection using indium phosphide quantum dots

Ilsong Lee,[‡a] Jieun Moon,[‡b] Hoomin Lee,[‡c] Sungjun Koh,[a] Gui-Min Kim,[a] Laure Marie Colette Gauthé,[a] Francesco Stellacci,[d] Yun Suk Huh,*[c] Pilhan Kim,*[be] and Doh C. Lee*[a]

[a]Department of Chemical and Biomolecular Engineering, Korea Advanced Institute of Science and Technology (KAIST), Daejeon 34141, Korea

[b]Graduate School of Nanoscience and Technology, KAIST, Daejeon 34141, Korea

[c]NanoBio High-Tech Materials Research Center, Department of Biological Engineering, Inha University, Incheon 22212, Korea

[d]Institute of Materials Science & Engineering, École Polytechnique Fédérale de Lausanne (EPFL), Lausanne 1015, Switzerland

[e]Graduate School of Medical Science and Engineering, KAIST, Daejeon 34141, Korea

*Corresponding author. Email: yunsuk.huh@inha.ac.kr (Y.S.H.); pilhan.kim@kaist.ac.kr (P.K.); dclee@kaist.edu (D.C.L.)

‡These authors contributed equally to this work.

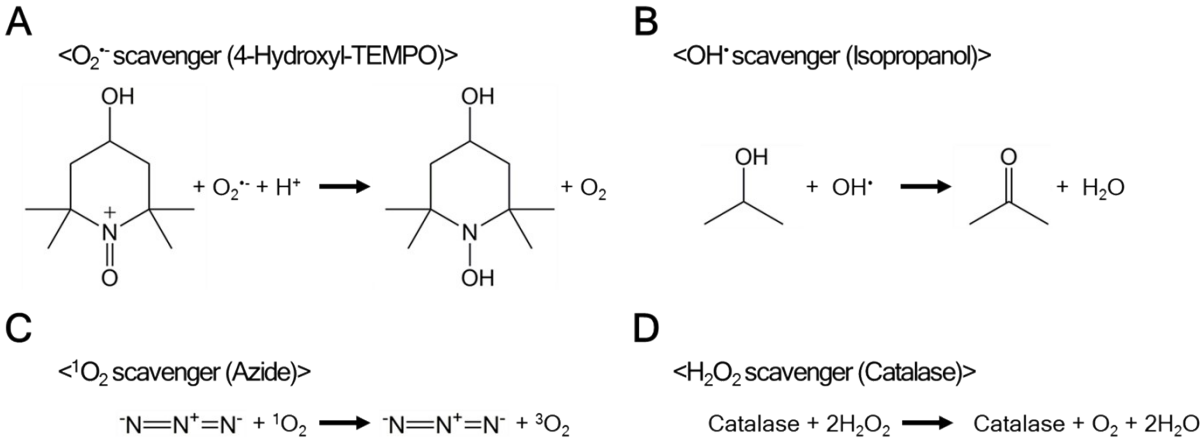

Figure S1. ROS scavenging mechanism of (A) 4-hydroxyl-TEMPO ($O_2^{\bullet-}$ scavenger), (B) isopropanol ($OH^{\bullet}$ scavenger), (C) azide ($^1O_2$ scavenger) and (D) catalase (H_2O_2 scavenger).

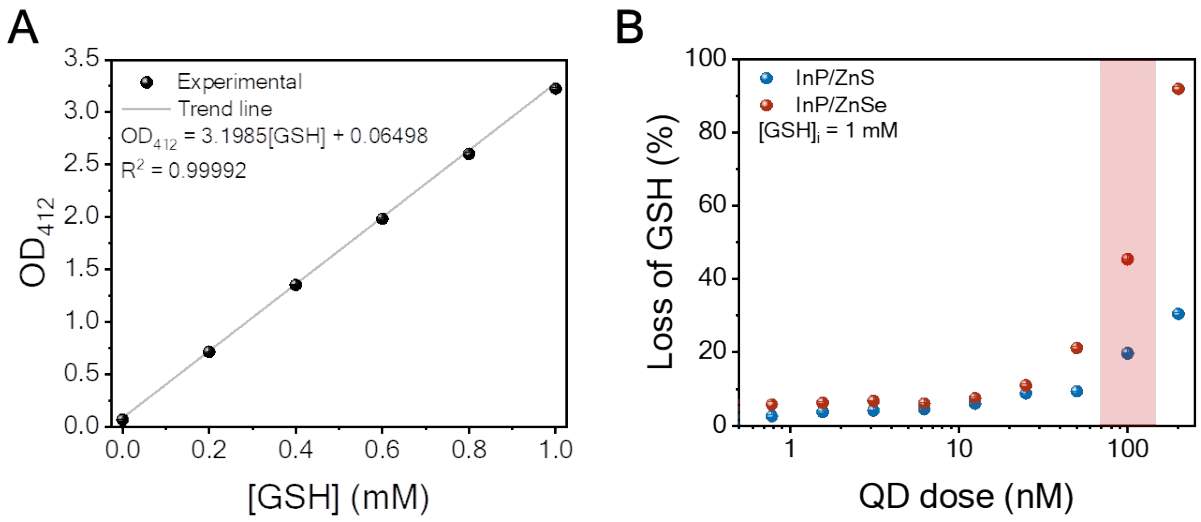

Figure S2. (A) Calibration curve for the quantification of glutathione (GSH) by Ellman's assay. (B) GSH oxidation of the InP QDs with different concentrations incubated for 1 hr.

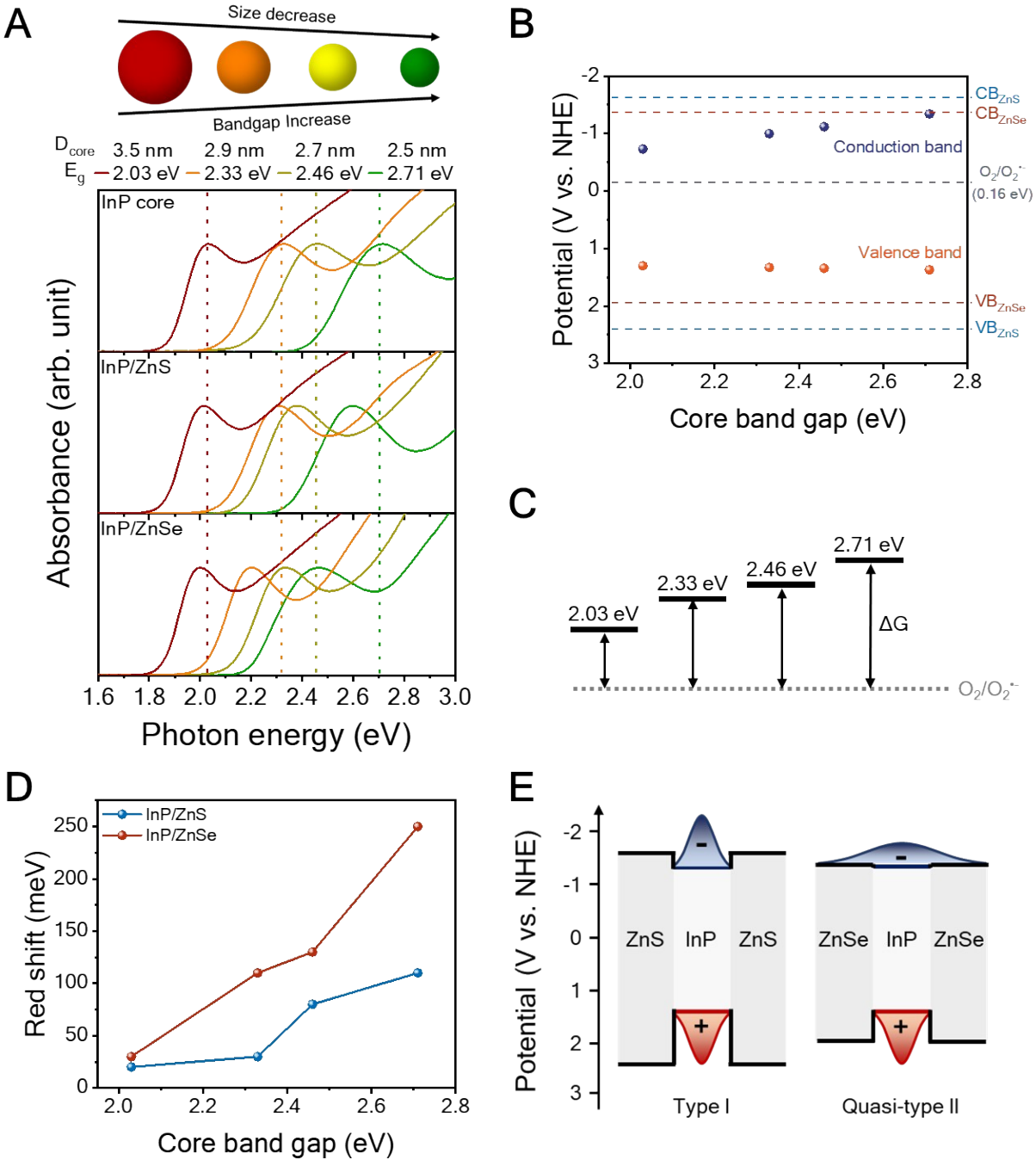

Figure S3. (A) Absorption spectrum of InP QDs with various core band gaps. (B) Band edge position of various size of InP cores and ZnS and ZnSe shells. (C) Schematic illustration of ΔG for superoxide generation of a variety of InP core band gaps. (D) Band gap red shift of InP QDs after zinc chalcogenide shell (2 monolayer) passivation. (E) Schematic illustration of the carrier localization of InP QDs.

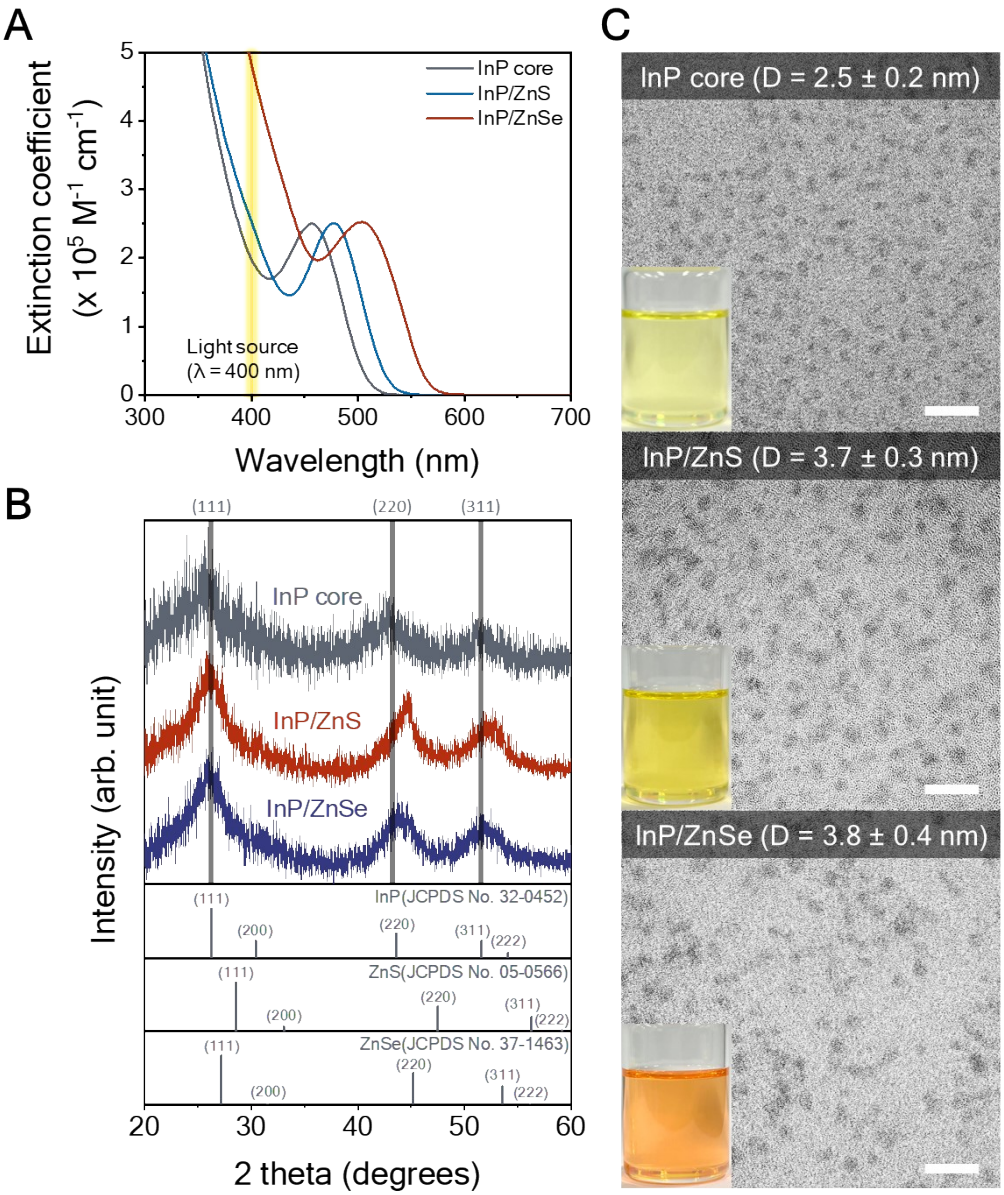

Figure S4. (A) Absorption spectra of InP core, InP/ZnS and InP/ZnSe. (B) X-ray diffraction (XRD) patterns of InP core, InP/ZnS and InP/ZnSe QDs. (C) Transmission electron microscopy (TEM) image of InP core, InP/ZnS and InP/ZnSe QDs with the average size of 2.5, 3.7 and 3.8 nm, respectively (The insets present photographs of solution of InP core, InP/ZnS and InP/ZnSe QDs.). The scale bars represent 10 nm.

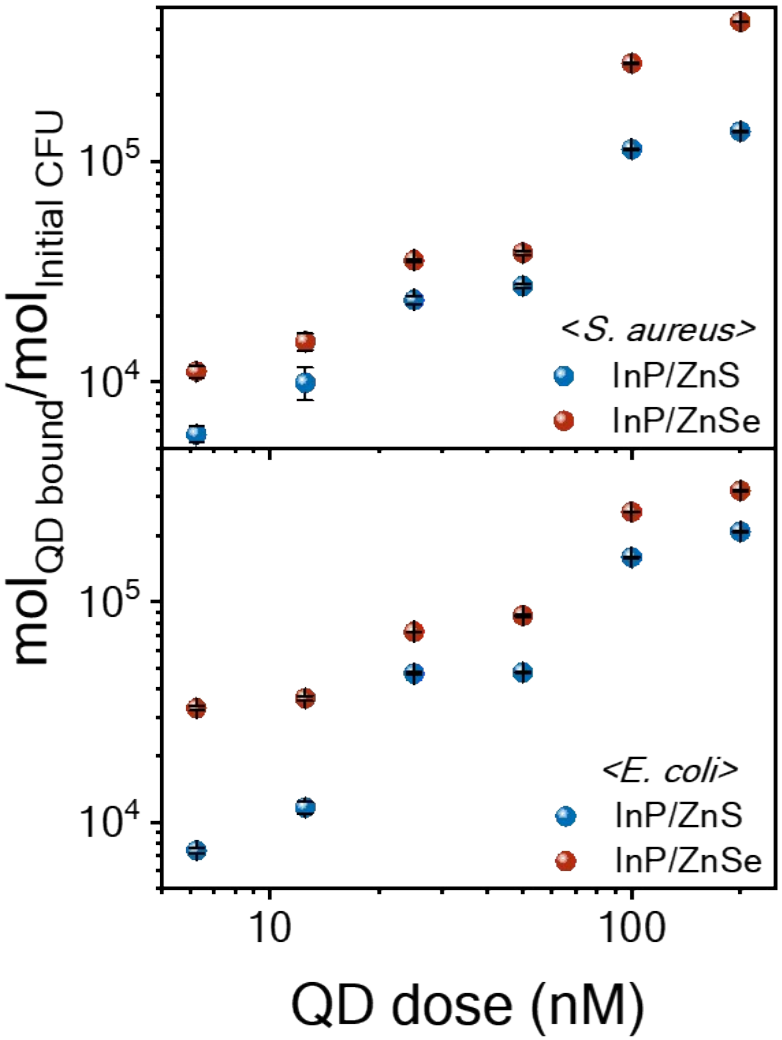

Figure S5. Number of bound QDs per cell of MDR *S. aureus* (upper panel) and *E. coli* (lower panel) at varying QD doses.

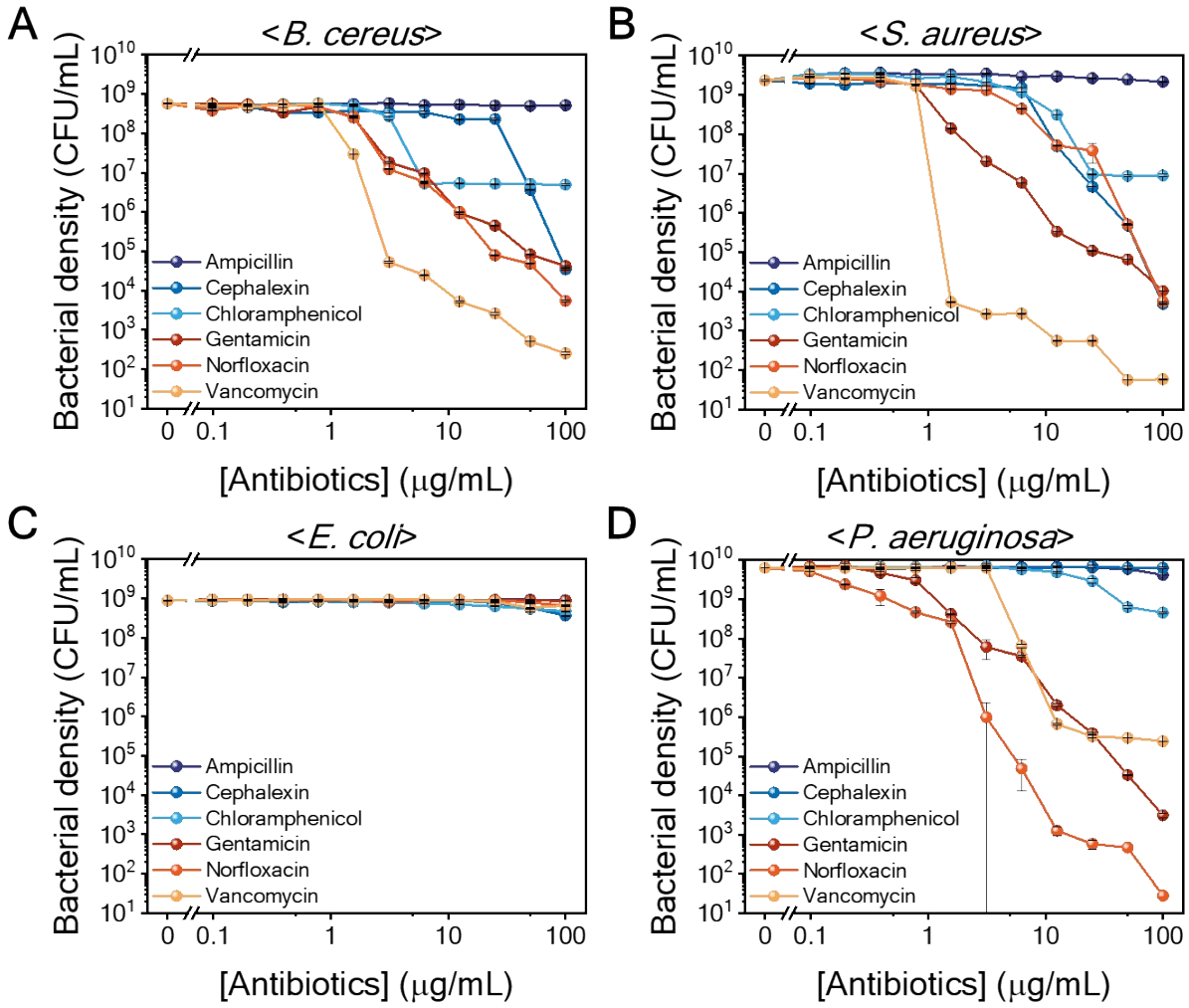

Figure S6. Colony-forming unit assay of (A) MDR *B. cereus*, (B) *S. aureus*, (C) *E. coli* and (D) *P. aeruginosa* incubated with different concentrations of a variety of antibiotics for 8 hr.

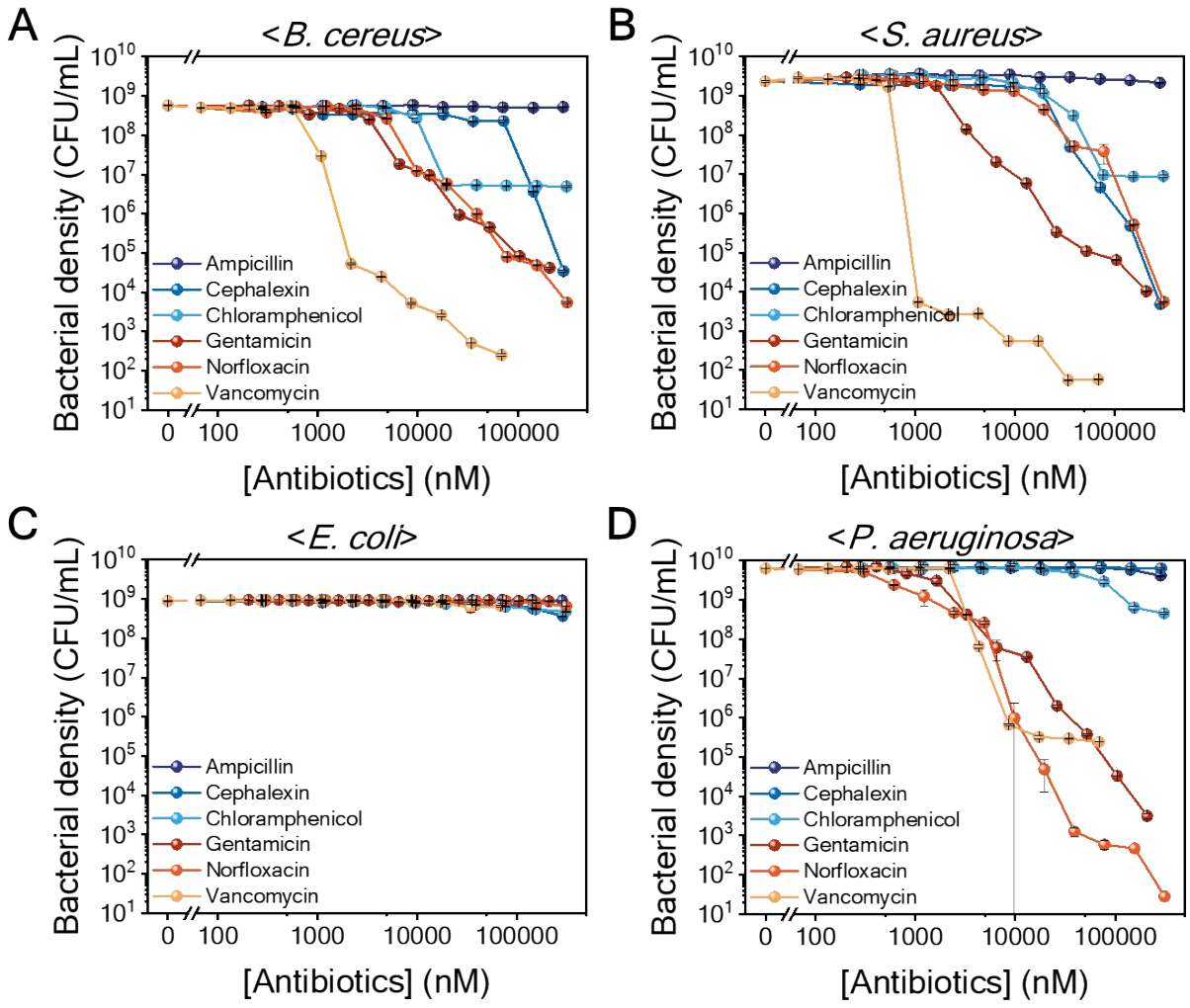

Figure S7. Modification of Figure S6 by changing x-axis unit from μg/mL to nM.

Table S1. Maximum values of minimal inhibitory concentration (MIC) of antibiotics on MDR *B. cereus*, *S. aureus*, *E. coli* and *P. aeruginosa* corresponding to Clinical and Laboratory Standard Institute 2020 breakpoint and the antibiotic treatment concentration in Figure S6

	AMP	**CEX**	**CHL**	**GEN**	**NOR**	**VAN**	**InP/ZnS**	**InP/ZnSe**
Minimal inhibitory concentration (μg/mL)	8	4	16	4	4	2	-	-
Treatment concentration (μg/mL)	12.5	6.25	25	6.25	6.25	3.125	0.4 (10 nM)	0.5 (10 nM)

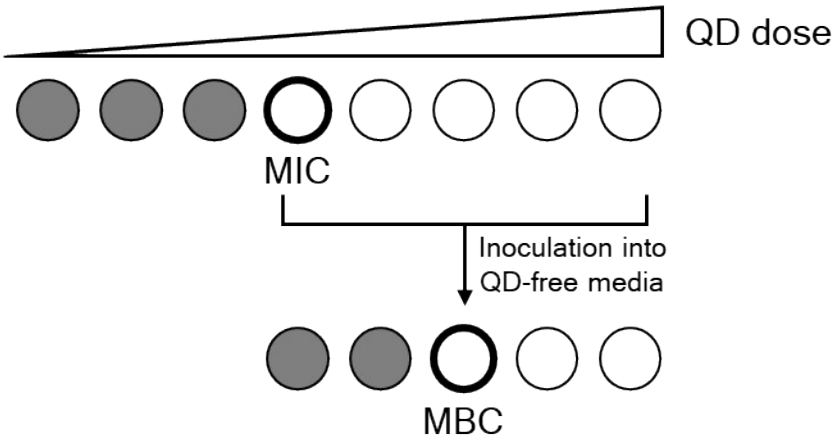

Figure S8. Schematic illustration of dilution method used to determine the minimal inhibitory concentration (MIC) and minimal bactericidal concentration (MBC).

Table S2. MIC and MBC values of InP/ZnSe QDs for MDR *S. aureus* and *E. coli*

		Bacterial density (CFU/mL)							
		10^1	**10^2**	**10^3**	**10^4**	**10^5**	**10^6**	**10^7**	**10^8**
S. aureus	MIC (nM)	0.25	0.25	0.25	0.25	1	4	8	85.3
	MBC (nM)	1	1	1	1	2	8	16	256
	MBC/MIC	4	4	4	4	2	2	2	4
E. coli	MIC (nM)	1	1	1.3	2	5.3	10.7	53.3	256
	MBC (nM)	4	4	5.3	8	16	42.7	128	1024
	MBC/MIC	4	4	4	4	3	4	2.4	4

Table S3. Therapeutic index of InP QDs on MDR *S. aureus* and *E. coli*

	InP/ZnS			**InP/ZnSe**		
	EC_{50}	**CC_{50}**	**TI**	**EC_{50}**	**CC_{50}**	**TI**
S. aureus	14 nM	9.8 μM	700	5 nM	15 μM	3,000
E. coli	14 nM	9.8 μM	700	14 nM	15 μM	1,071

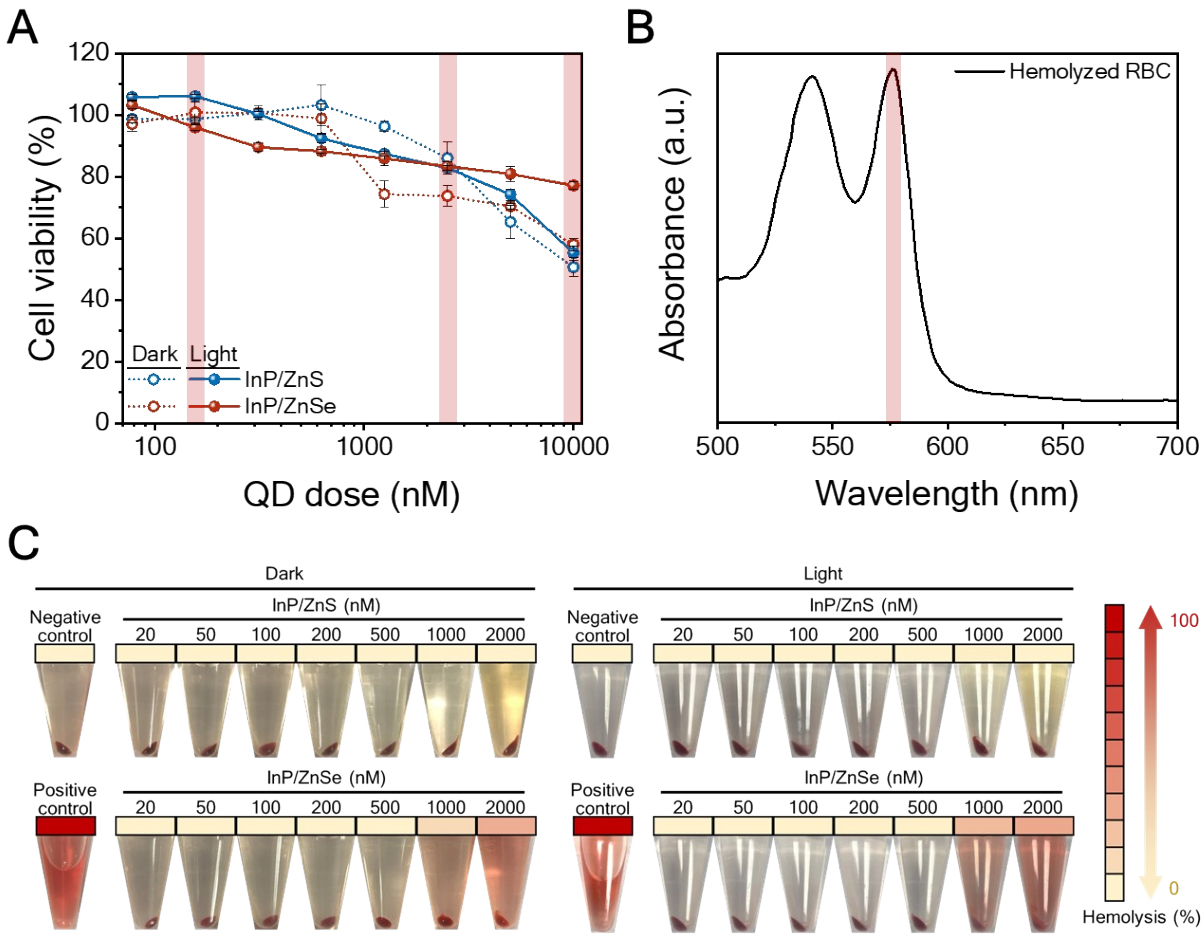

Figure S9. Biocompatibility evaluation of InP QDs. (A) Cytotoxicity of InP QDs determined by MTT cytotoxicity colorimetric assay in human keratinocyte (HaCaT) cells in the presence of InP QDs in dark or under 400 nm LED illumination. (B) Absorption spectra of hemolyzed mouse red blood cells (RBCs). (C) Photographs of fresh mouse RBCs incubated with Triton X-100 (positive control), PBS (negative control) and InP QDs with various concentration (20 to 2000 nM) in dark or under 400 nm LED illumination. Hemolysis ratio is presented in color heatmap.

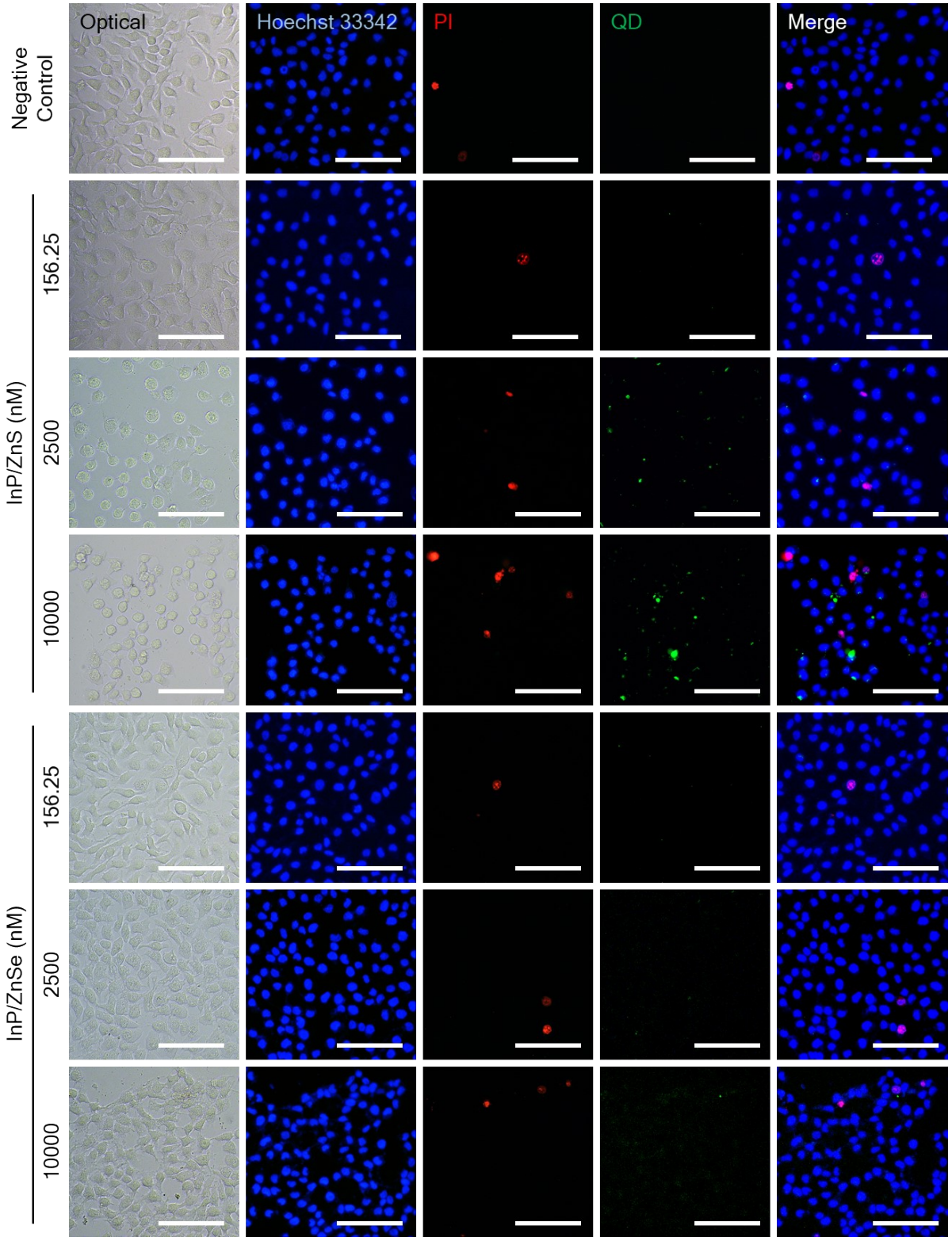

Figure S10. Hoechst 33342/PI double staining of HaCaT cells treated with InP QDs at the concentration of 156.25, 2500 and 10000 nM in dark. Scale bars represent 100 μm.

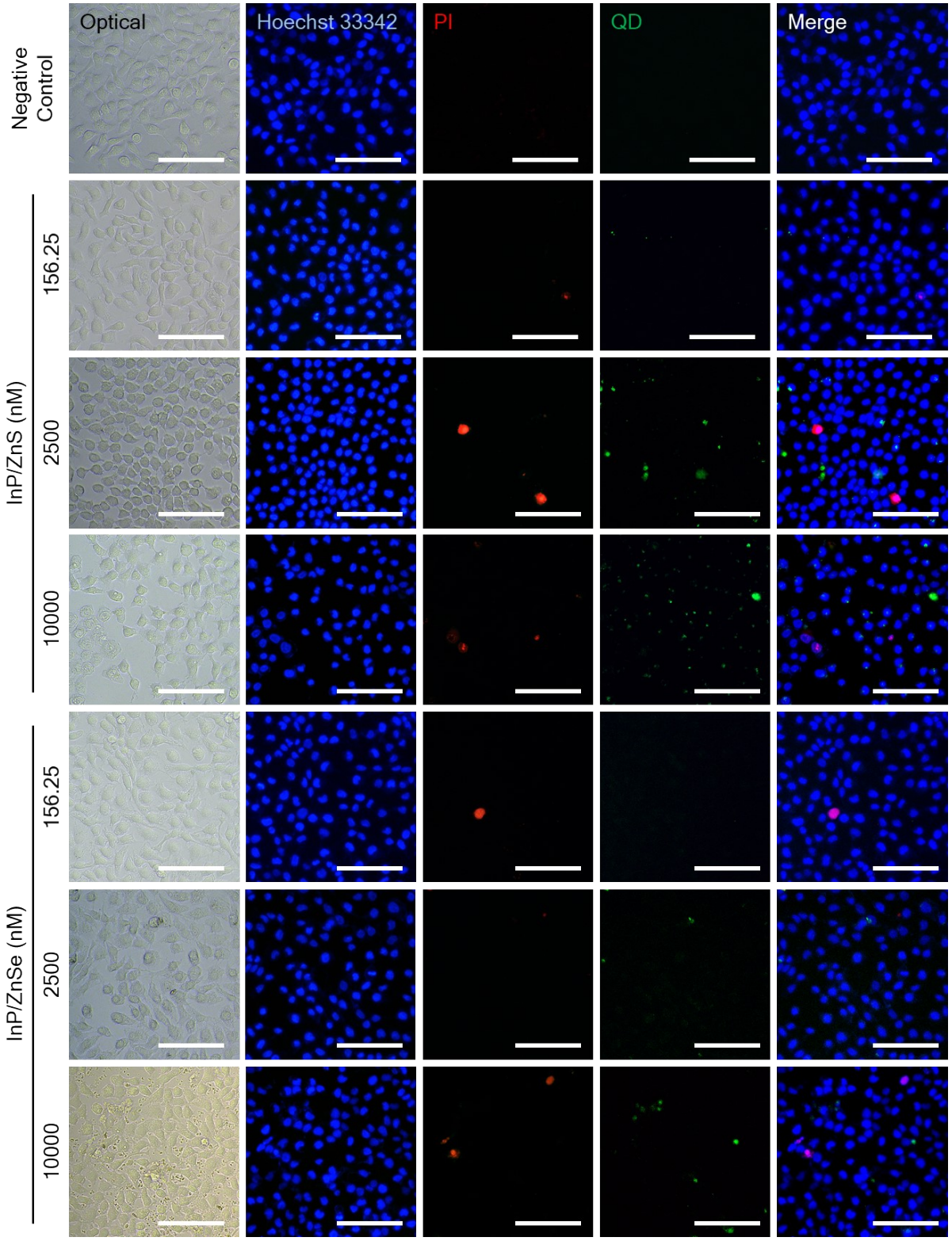

Figure S11. Hoechst 33342/PI double staining of HaCaT cells treated with InP QDs at the concentration of 156.25, 2500 and 10000 nM under 400 nm LED illumination (80 μW/cm^2). Scale bars represent 100 μm.

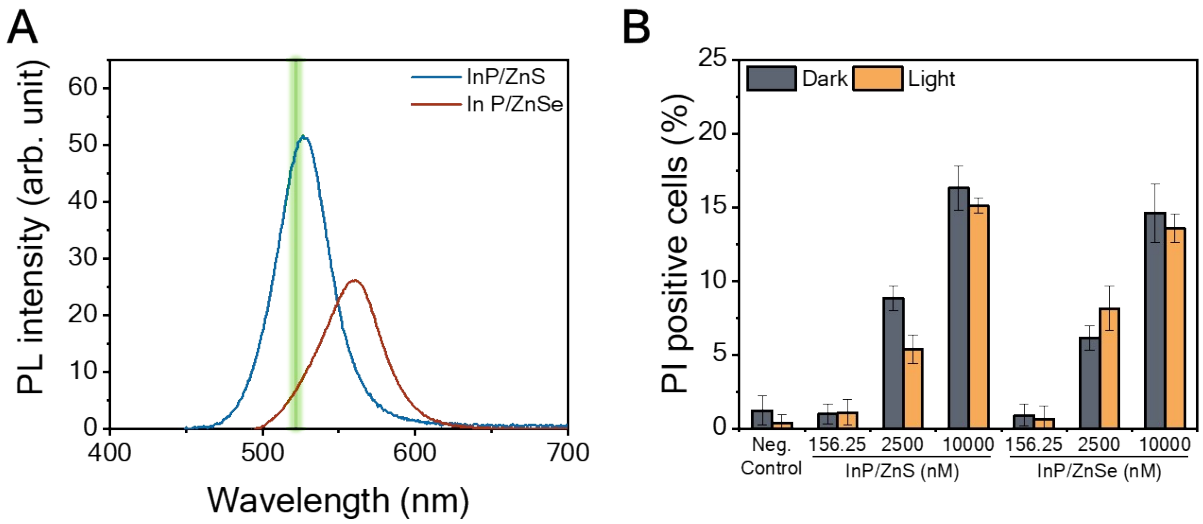

Figure S12. (A) . Photoluminescence (PL) spectra of InP QDs at the concentration of 1000 nM. (B) Ratio of PI positive HaCaT cells treated with InP QDs at the concentration of 156.25, 2500 and 10000 nM in dark and under light illumination.

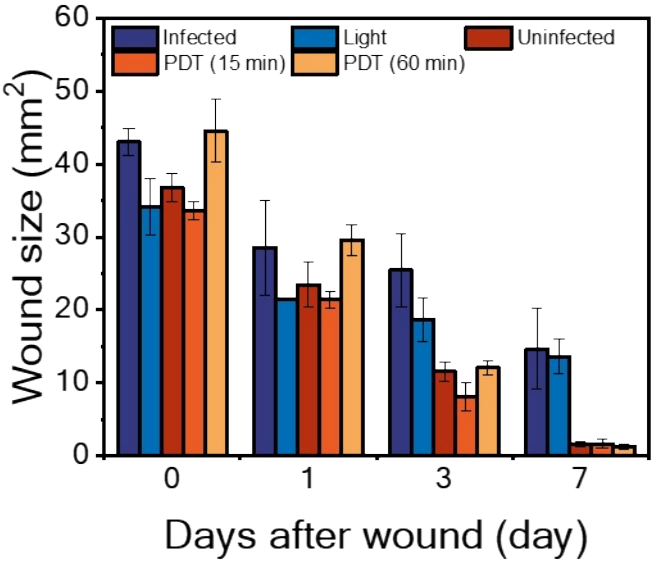

Figure S13. Change of the area sizes of wound during treatment (number of mice = 5). Error bars represent the standard deviation from quintuplicate experiments.

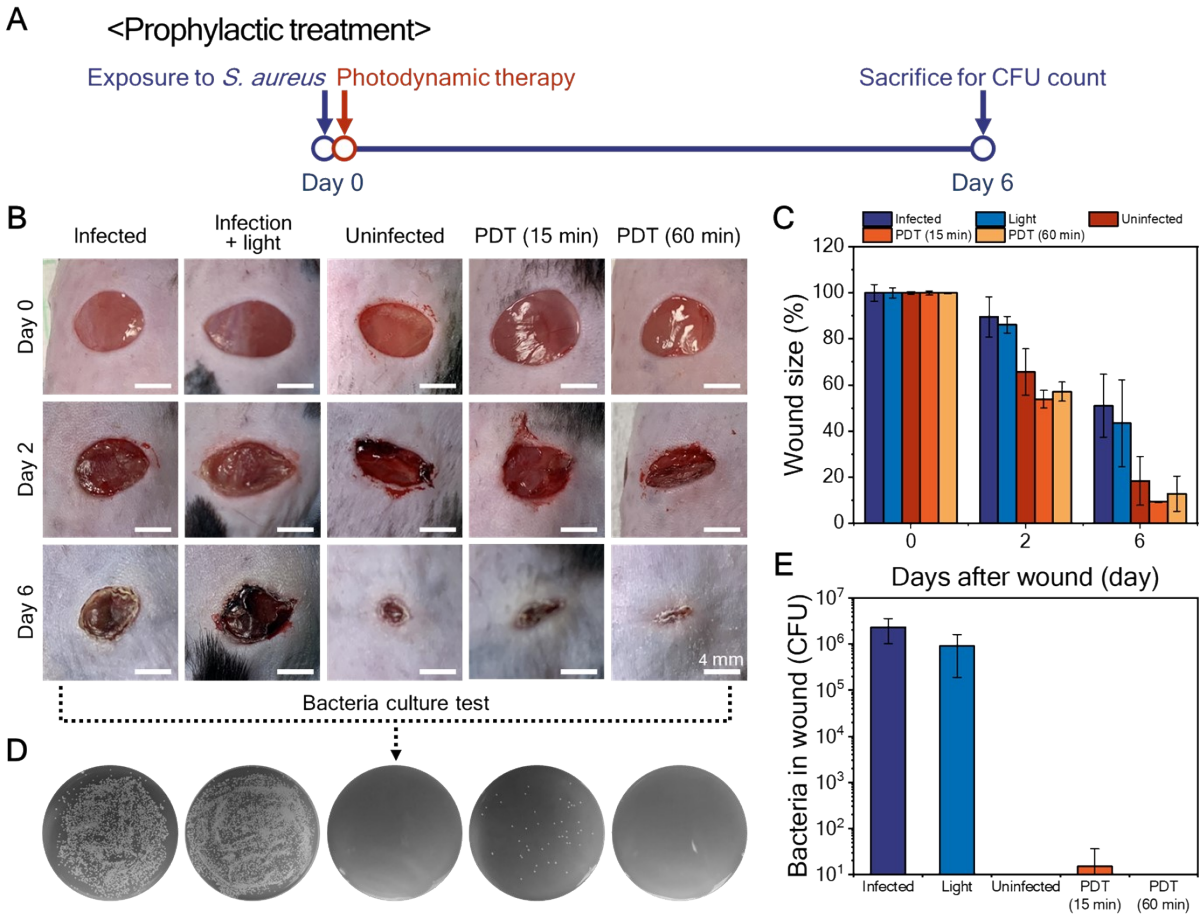

Figure S14. *In vivo* prophylactic treatment against MDR *S. aureus*-exposed wounds by InP/ZnSe QDs. (A) Schematic timeline of the curative procedure of skin infection. (B) Photographs of infected mice skin wound treated after different treatments. The scale bars represent 4 mm. (C) Changes of the wound size during treatment (number of mice = 5). (D) Photographs of agar plate of the number of bacteria in skin wound on day 6. (E) Number of surviving bacteria in skin wound on day 6.